



Full Length Article

Determination of physicochemical properties of biodiesel and blends using low-field NMR and multivariate calibration



André F. Constantino^a, Diana C. Cubides-Román^a, Reginaldo B. dos Santos^a, Luiz H.K. Queiroz Jr.^b, Luiz A. Colnago^c, Álvaro C. Neto^a, Lúcio L. Barbosa^d, Wanderson Romão^e, Eustaquio V.R. de Castro^a, Paulo R. Filgueiras^a, Valdemar Lacerda Jr.^{a,*}

^a Federal University of Espírito Santo, Postgraduate Program in Chemistry, Av. Fernando Ferrari 514, Goiabeiras, 29075-073 Vitória, ES, Brazil

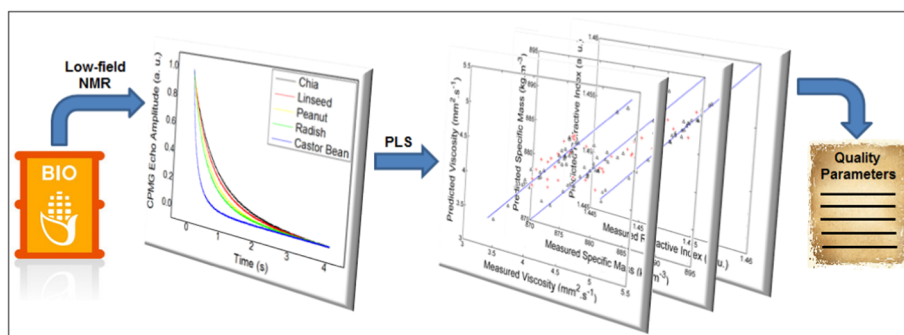
^b Federal University of Goiás, Institute of Chemistry, Av. Esperança s/n, Chácara Califórnia, 74690-900 Goiânia, GO, Brazil

^c Embrapa Instrumentation, Rua 15 de Novembro 1452, Centro, 13560-970 São Carlos, SP, Brazil

^d Federal University of São Paulo, Department of Marine Sciences, Rua Silva Jardim 136, Vila Matias, 11015-020 Santos, SP, Brazil

^e Federal Institute of Education, Science and Technology of Espírito Santo, Av. Ministro Salgado Filho 1000, Soteco, 29106-010 Vila Velha, ES, Brazil

GRAPHICAL ABSTRACT



ARTICLE INFO

Keywords:

Biodiesel
Low-field NMR
PLS
Kinematic viscosity
Specific mass
Refractive index

ABSTRACT

Because the methods specified by regulatory agencies for the determination of the physicochemical properties of biodiesel can be laborious and expensive, the development of alternative methodologies represents a major breakthrough. Thus, low-field nuclear magnetic resonance (NMR) is an advantageous option because it is nondestructive and reduces the cost and time consumption. In this study, the partial least squares (PLS) regression method was used to create models that correlated the decay curves of the Carr–Purcell–Meiboom–Gill (CPMG) signal, obtained from low-field NMR equipment (2.2 MHz for ¹H), with the kinematic viscosity, specific mass and refractive index of biodiesel and their blends. Seventeen oilseeds diversified between edible and non-edible oils were utilized to synthesize the biodiesel and produce binary blends. Separately, multivariate calibration models were created only with biodiesel and blends with castor bean because these samples showed different tendencies from the others. The values of root mean square error of prediction (RMSEP) for the kinematic viscosity, specific mass and refractive index were equal to $0.1 \text{ mm}^2\text{s}^{-1}$, $3.7 \text{ kg}\cdot\text{m}^{-3}$ and 0.002, re-

* Corresponding author.

E-mail address: vljuniorqui@gmail.com (V. Lacerda).

<https://doi.org/10.1016/j.fuel.2018.10.045>

Received 22 April 2018; Received in revised form 30 August 2018; Accepted 6 October 2018

Available online 15 October 2018

0016-2361/ © 2018 Elsevier Ltd. All rights reserved.

spectively, for samples of biodiesel and blends without castor bean and $0.6 \text{ mm}^2\text{s}^{-1}$, $2.0 \text{ kg}\cdot\text{m}^{-3}$ and 0.0005 for samples of biodiesel and blends with castor bean. The results reveal that the developed models are very satisfactory to predict the quality parameters of biodiesel and blends based on CPMG data with fairly good efficacy.

1. Introduction

Chemically, biodiesel is composed of monoalkyl esters of long chain fatty acids derived from renewable feed stocks, such as vegetable oil or animal fats, that are synthesized by transesterification, in which the triglycerides in vegetable oils react with alcohols of low molecular weights in the presence of catalysts [1–2]. Biodiesel presents several interesting features that tend to highlight it as an excellent alternative fuel source as a partial or complete replacement for diesel. Among these characteristics, it should be emphasized that its production is environmentally acceptable, technically feasible, and economically competitive and can promote social development, in addition to its raw materials being readily available [2–8].

The quality of biodiesel is related to several properties, such as ignition quality, heat of combustion, cold flow, oxidative stability, viscosity, specific mass, and lubricity [9]. Viscosity affects the atomization of a fuel after injection into the combustion chamber and consequently the formation of engine deposits. The higher the viscosity is, the greater the tendency of the fuel to cause such problems [10,11]. Specific mass is related to many engine performance characteristics, such as cetane number and heating value. Moreover, diesel fuel injection systems measure the fuel by volume. Thus, changes in the fuel density will influence the engine output power due to the different masses of fuel injected [12]. The refractive index is also an important physicochemical property that is widely used in fuel characterization and may be used to indicate the presence of a microemulsion during the biodiesel production process [13].

The methods specified by regulatory agencies for the evaluation of such parameters are in many cases, laborious, expensive and destructive to the sample, as can be verified through the requirements of the ANP (Brazilian National Agency for Petroleum, Natural Gas and Biofuels) [14]. In this sense, low-field ^1H NMR relaxometry has already been shown as an alternative method in studies of oil content and oil quality in oilseeds [15] and in the evaluation of biodiesel quality [9].

Low-field NMR (or time-domain nuclear magnetic resonance – TD-NMR), which is called as such because of the low magnetic field applied ($B_0 < 1 \text{ T}$), is based on less-expensive, small, and robust benchtop permanent low-field magnets, which significantly reduces the overall system and running costs. The technique has been proven to be an excellent alternative to many traditional methods because of its rapidity, reproducibility, high correlation with these traditional methods, possibility for *online* and *in situ* application, non-destructiveness and minimal or absent sample pre-treatment requirements [16]. For these reasons, low-field NMR has been widely used for qualitative and quantitative analyses [15–38]. Experiments are performed mainly by using the difference in longitudinal relaxation time (T_1), transverse relaxation time (T_2) (relaxometry) or self-diffusion (D , diffusometry) between the sample constituents [16].

In measurements on low-field NMR equipment, the Carr–Purcell–Meiboom–Gill (CPMG) pulse sequence [39] stands out as the most important sequence. It has been used in analyses of seed, vegetable oil and foodstuffs, replacing laborious processes that consume toxic organic chemicals [15,19–31], in the petroleum industry in well-logging sensors and in the laboratory to measure oil viscosity, density, rock porosity and many other properties for the oil industry [16,32–38].

NMR data can also be modelled using chemometric methods, such as principal component analysis (PCA), hierarchical cluster analysis (HCA) and partial least squares (PLS) regression, which is one of the most widely used methods for creating calibration models [9,15,40].

To provide only one property (PLS-1), the PLS algorithm searches for a set of components that explain the maximum covariance between the

dependent (\mathbf{X}) and independent variables (\mathbf{y}). It is reached by the simultaneous decomposition of the set of instrumental data (\mathbf{X}) and of the physicochemical property (\mathbf{y}) obtained by traditional method, followed by a regression model relating the two decomposition models [13,41–43]. In PLS regression the matrix \mathbf{X} and the vector \mathbf{y} are simultaneously decomposed as the covariance structure between them is maximized.

$$\mathbf{X} = \mathbf{TP}^t + \mathbf{E}_x \quad (1)$$

$$\mathbf{y} = \mathbf{Uq}^t + \mathbf{e}_y \quad (2)$$

where \mathbf{T} and \mathbf{U} are the score matrices and \mathbf{P}^t and \mathbf{q}^t are the transposed weight matrix and the transposed weight vector of the matrix \mathbf{X} and of the vector \mathbf{y} , respectively. \mathbf{E}_x and \mathbf{e}_y are the residual matrix and residual vector containing the unexplained variances of \mathbf{X} and \mathbf{y} , respectively [13,41–43]. The inner relationship between the score matrices \mathbf{T} and \mathbf{U} is given by the equation:

$$\mathbf{b} = \mathbf{W}(\mathbf{P}^t\mathbf{W})^{-1}\mathbf{q} \quad (3)$$

where \mathbf{b} is the vector of the regression coefficients and \mathbf{W} is a weights matrix for loadings from \mathbf{X} [41].

Thus, in this paper, the low-field ^1H NMR technique associated with partial least squares (PLS) regression method was used to estimate the kinematic viscosity, specific mass and refractive index of biodiesel samples and their blends.

2. Material and methods

2.1. Studied biodiesel

Table 1 presents the edible and non-edible oils used for biodiesel synthesis. These oils have similar fatty acids variability of the oils/fats used in commercial biodiesel production.

2.2. Low-field NMR analysis

The low field NMR equipment used in the analysis of biodiesel and blends samples was a MARAN Ultra-2 from Oxford Instruments, which was operated at 52 mT (2.2 MHz for ^1H) conducted by a probe of 51 mm in diameter and controlled by the Oxford Instruments RINMR software. The measurement temperature was equal to $35.0 \pm 0.5^\circ\text{C}$.

Table 1
Oilseeds selected for synthesis of biodiesel.

Common Names	Scientific Names
Pumpkin	<i>Cucurbita pepo</i> L.
Cottonseed	<i>Gossypium hirsutum</i> L.
Peanut	<i>Arachis hypogaea</i> L.
Canola	<i>Brassica napus</i> L.
Safflower	<i>Carthamus tinctorius</i> L.
Chia	<i>Salvia hispanica</i> L.
Cutieira	<i>Joannesia princeps</i> Vell
Palm	<i>Elaeis guineensis</i> Jacq.
Sesame	<i>Sesamum indicum</i> L.
Sunflower	<i>Helianthus annuus</i> L.
Linseed	<i>Linum usitatissimum</i> L.
Castor Bean	<i>Ricinus communis</i> L.
Watermelon	<i>Citrullus lanatus</i> L.
Corn	<i>Zea mays</i> L.
Radish	<i>Raphanus sativus</i> L.
Candlenut	<i>Aleurites moluccana</i> L.
Soybean	<i>Glycine max</i> L.

The CPMG pulse sequence employed 90° and 180° pulses of 8.6 and 17.2 μs , τ of 100 μs and recycle delay of 5 s. The maximum intensity of 10,240 even echoes was acquired and average with 32 transients.

2.3. Oil extraction

In the first step of analysis, the extraction of the oil from the oilseeds samples selected for the study, using hexane as the extracting solvent was performed. The system was refluxed for 6 h and the resulting extracted solution was dried over anhydrous sodium sulfate to remove traces of free water. After filtering the solution, the solvent was removed on a rotary evaporator, and the mass of extracted oil was weighed.

2.4. Transesterification and analysis of biodiesel samples

For biodiesel synthesis, sodium hydroxide (NaOH) was used as the reaction catalyst. The mass of sodium hydroxide used was 1% of the mass of oil, and NaOH was pre-solubilized in methanol under vigorous stirring and then added to a round bottom flask containing the vegetable oil. After addition, a reflux condenser was connected to the flask, which was in a glycerin thermal bath and under constant magnetic stirring. The molar ratio of oil:methanol was 1:6, and the reaction occurred within the temperature range of 55–60 $^\circ\text{C}$ for 30 min.

To follow the end of the reaction, the thin layer chromatography method was used. The elution solvent was a mixture of hexane, ethyl ether and acetic acid in a ratio of 85:15:1 (v/v/v). Visualization was performed in an iodine chamber.

The reaction product was placed in a separation funnel where glycerin, a by-product of the reaction, was separated from the biodiesel by decantation. Then, the biodiesel was washed several times with hot water until the pH became neutral, and after it was transferred to an Erlenmeyer flask where anhydrous sodium sulfate was added as a drying agent. Subsequently, the product was filtered into a storage vessel.

Finally, approximately 25 g of the biodiesel samples were analyzed three times by CPMG, and a mean decay curve was generated.

2.5. Preparation and analysis of the biodiesel blends

The formulation of biodiesel blends can be an excellent option to adapt the physicochemical properties of a given matrix to the current norms or even to modify some interesting specific properties. In addition, when the range of oilseeds used by a country for the synthesis of biodiesel is diversified, blends are also an excellent alternative to bypass market or production problems in order to obtain the needed amount of biodiesel.

Therefore, binary blends of linseed/peanut, chia/radish, sunflower/palm and canola/cotton were prepared at ratios of 10:90, 25:75, 50:50,

75:25 and 90:10, and castor bean/soybean blends were produced at ratios of 10:90, 20:80, 30:70, 40:60, 50:50, 60:40, 70:30, 80:20 and 90:10. Approximately 25 g were also analysed three times by CPMG to obtain a mean decay curve.

It is important to clarify that the sunflower/palm, canola/cotton and castor bean/soybean blends were produced with biodiesel synthesized from commercially available oils. In these cases, pure biodiesel was also analyzed by CPMG.

2.6. Determination of physicochemical properties

The following quality parameters of the biodiesel and the blends were then determined: kinematic viscosity, specific mass and refractive index.

The kinematic viscosity at 40 $^\circ\text{C}$ of the samples was obtained in duplicate according to the ASTM D445 method. The experiments were performed on a SCHOTT automatic viscometer, model AVS350, equipped with a digital thermostatic bath for temperature control in which a Cannon-Fenske type 150 capillary tube with 10 mL of the sample was used.

The determination of the specific mass at 20 $^\circ\text{C}$ was performed in duplicate using an Anton Paar DMA-5000 digital densimeter according to ASTM D4052. The refractive indices were measured at 25 $^\circ\text{C}$ in an Abbe Digital refractometer (Krüss, Germany, model AR 2008).

2.7. Partial least squares (PLS)

Matlab® software version 7 (Mathworks Inc.) was used to build the partial least squares regression (PLS) models of the CPMG signals of the biodiesel and blends samples obtained from MARAN equipment.

The PLS models were created based on the selection of the intensity values of the first 5120 echoes of each matrix by allocating them in 5120 columns. These values were preprocessed by centring them on the mean, i.e., each intensity value of a given column was subtracted from the mean intensity value of the given column. The dataset was split into calibration (70% of the samples) and prediction (30% of the samples) sets. The calibration set was used to build the calibration model, which was then applied to the prediction set.

Calibrations were performed by leave-one-out cross-validation (one at a time, each sample was removed from the calibration set and tested in the model constructed with the others) to determine the optimal number of latent variables (LV) to be included in each model in order to minimize the root mean square cross-validation error (RMSECV), which was also calculated from Eq. (4) but using an n equal to the number of calibration samples. The PLS model adjustments were evaluated by correlating the predicted values with the reference values of the validation set in a graph. To evaluate and compare the accuracy of the PLS

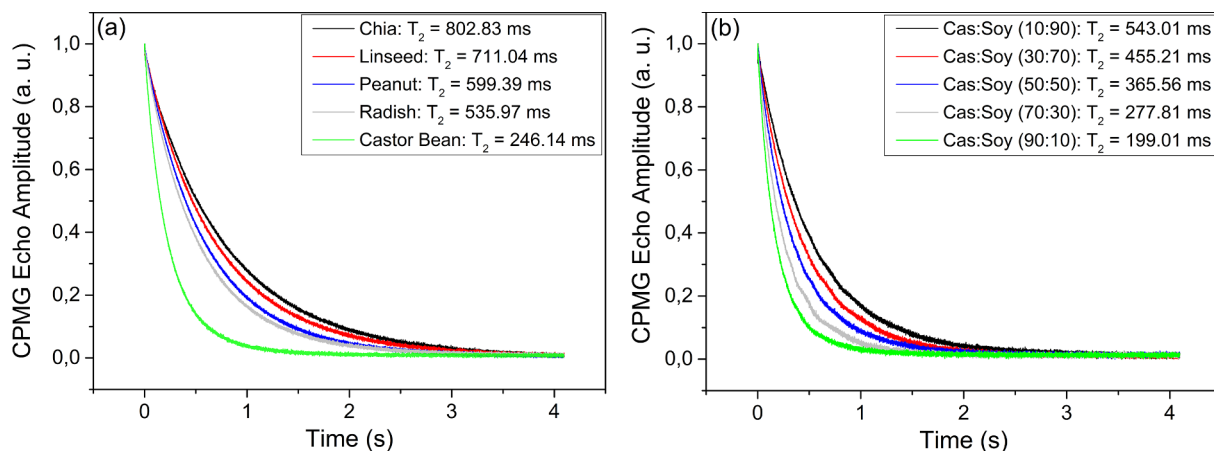


Fig. 1. Normalized decay curves of the CPMG signal of the analysed samples according to their category: (a) pure biodiesels; and (b) biodiesel blends of Cas:Soy.

models created, root mean square error of prediction (RMSEP) was calculated according to Eq. (4). RMSEP is an excellent statistical parameter that measures how well the generated model manipulates new samples [13,42–44].

$$RMSEP = \sqrt{\frac{\sum_{i=1}^n (y_i - \hat{y}_i)^2}{n}} \quad (4)$$

where \hat{y}_i and y_i are the predicted and the reference values of the i th sample, respectively, and n is the number of prediction samples.

The PLS models constructed for the determination of the physicochemical properties of pure biodiesel and blends with castor bean were developed using the repeated double cross-validation (RDCV) algorithm [45,46]. This process is recommended when the number of samples existing for model construction is limited and is called as such because it is applied two times to estimate a set of samples. In RDCV, the calibration and validation sets are divided k -times, and k PLS models are constructed. The PLS model is constructed with calibration samples and applied to estimate the physicochemical property in the validation set.

3. Results and discussion

3.1. Interpretation CPMG signals

Fig. 1 shows the normalized decay signals for some analyzed samples of pure biodiesel (a) and biodiesel blends of Cas:Soy (b). It can be seen that the curves with faster decay have lower values of T_2 , which were calculated from a mono-exponential fitting. There is an inverse correlation between the viscosity of the biodiesel and their values of T_2 , which is shown later in Figs. 2a and 3a, and can be explained by the correlation time of the molecules (τ_c). The correlation time is defined as the average time required for the molecule to rotate through an angle of 1 rad around any axis [47]. The most viscous samples contain molecules with the highest of τ_c values and have short T_2 . However, the less viscous samples contain molecules with short τ_c , so their T_2 values will be longer.

Then, in Fig. 1a, the longer decay of chia biodiesel ($T_2 = 802.83$ ms) indicates its low viscosity ($3.7163 \text{ mm}^2 \cdot \text{s}^{-1}$). On the other hand, the castor bean biodiesel, with much shorter decay (lower value of T_2) is the most viscous biodiesel ($12.2782 \text{ mm}^2 \cdot \text{s}^{-1}$). Fig. 1b shows the CPMG decays of castor bean:soybean (CAS:SOY) blends, which also represent the other blends. It is clear that the higher the proportion of the most viscous biodiesel in the blend is (in this case, castor bean), the lower the T_2 value of the sample, and the faster the decay.

3.2. Obtained physicochemical properties

Table S1, given as Supplementary material, shows the values of physicochemical parameters obtained, as well as the error of each measure.

The kinematic viscosity range accepted by the ANP is from 3.0 to $6.0 \text{ mm}^2 \cdot \text{s}^{-1}$, so only the two castor biodiesel samples (synthesized from oil extracted and commercial) and the blends in which the percentage of castor bean biodiesel is equal to or greater than 40% did not comply with the norm. The values are even much higher than that allowed by the regulatory agency (reaching $15.5 \text{ mm}^2 \cdot \text{s}^{-1}$) and represent a great obstacle for castor bean biodiesel to be commercialized, even in blends. Castor oil produces a much more viscous biodiesel due to the presence more than 85% of ricinoleate in its composition. The hydroxyl group present on carbon 12 of this methyl ester, which is uncommon in other esters, increases the intermolecular hydrogen bonds and raises the oil viscosity [48,49].

The permitted range for the specific mass is between 850 and $900 \text{ kg} \cdot \text{m}^{-3}$. Thus, the same samples with nonconformity in viscosity were also non-compliant with regard to the specific mass. The only exception was the 40:60 castor bean/soybean blend, which was within

the allowed limit for the specific mass but did not conform to the range for kinematic viscosity.

The refractive index is not a physicochemical parameter required by the ANP; however, it is important to evaluate the biodiesel quality and can be interesting to include as a quality parameter for biodiesel characterization.

In addition to the non-compliance with the ANP-stipulated limits, biodiesel and castor bean blends present another difference in relation to the other samples: the correlations between the physicochemical properties and, consequently, with the T_2 values. Figs. 2 and 3 illustrate the correlations between the kinematic viscosity values (ν) and T_2 and

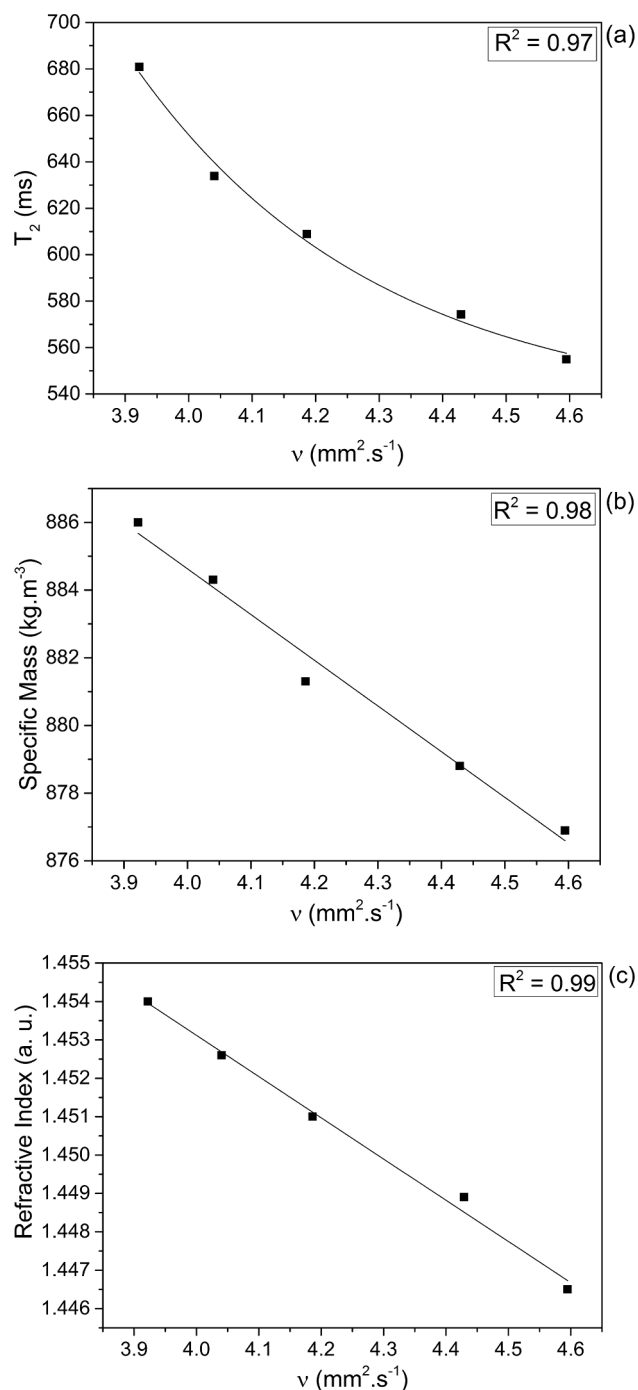


Fig. 2. Correlation curves between kinematic viscosity values (ν) of biodiesel blends of linseed/peanut (ratios of 10:90, 25:75, 50:50, 75:25 and 90:10) and: (a) T_2 ; (b) specific mass; and (c) refractive index. The peanut biodiesel is the most viscous.

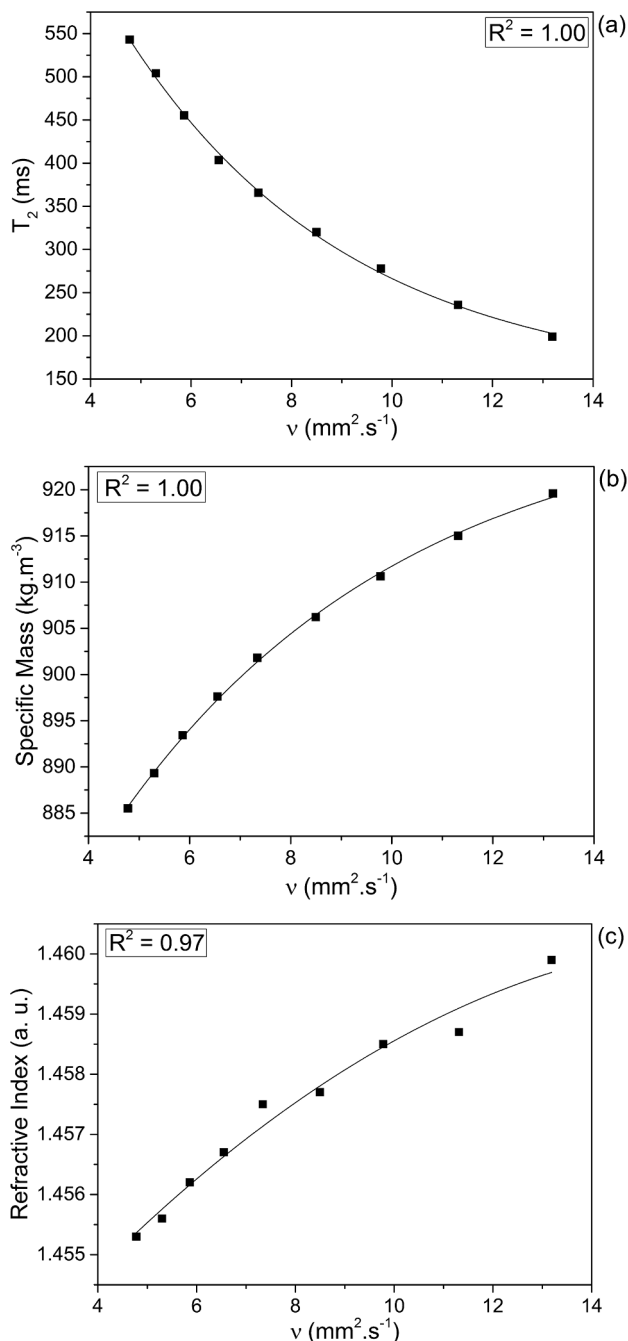


Fig. 3. Correlation curves between kinematic viscosity values (ν) of biodiesel blends of castor bean/soybean (ratios of 10:90, 20:80, 30:70, 40:60, 50:50, 60:40, 70:30, 80:20 and 90:10) and: (a) T_2 ; (b) specific mass; and (c) refractive index. The castor bean biodiesel is the most viscous.

the other quality parameters: as specific mass and refractive index. Fig. 2 shows the correlations of linseed/peanut blends, where peanut biodiesel is the most viscous, and Fig. 3 is the correlations of castor bean/soybean blends.

For the samples without castor bean there is an inverse correlation between the kinematic viscosity and the other physicochemical properties (Fig. 2). Fig. 2b and c show the linear correlation decreasing with high determination coefficients of specific mass and refractive index with viscosity, respectively. It is emphasized that as the viscosity presents an inverse correlation with T_2 (Fig. 4a), so the other parameters will have a direct correlation.

These inverse correlations can be explained from the composition of

methyl esters in biodiesel. The biodiesel viscosity increases with the increase in the ester chain size and decreases with the increase in the unsaturation degree [10–11], whereas for the other parameters the relation is different, they increase with the increase in unsaturation degree of biodiesel and a decrease in the length of the chains causes an increase in the specific mass and a decrease in the refractive index [50].

For biodiesel samples containing castor bean (Fig. 3) the curves are

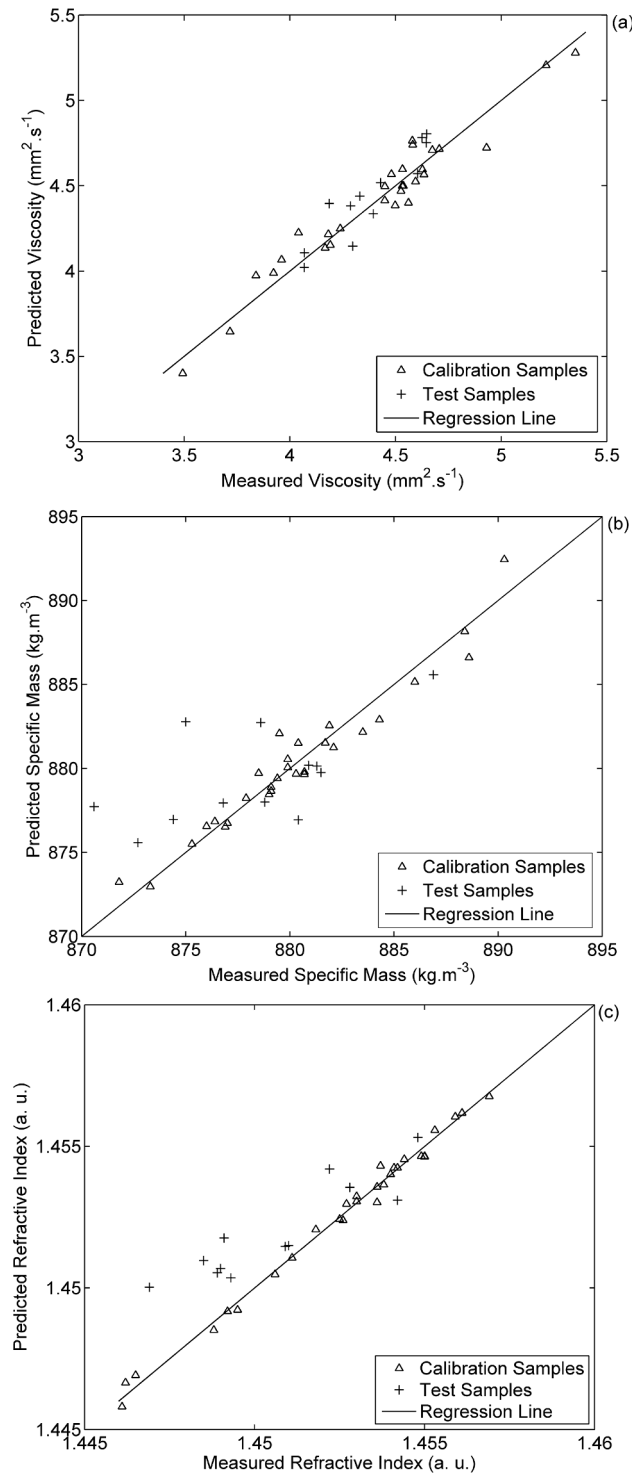


Fig. 4. Measured physicochemical properties by ASTM methods and its predicted values from the constructed PLS models: (a) viscosity; (b) specific mass; and (c) refractive index. The CPMG data used to build the models were generated from analyses of pure biodiesel and blends without castor bean.

in the opposite direction. There are direct correlations between the kinematic viscosity and the other parameters. The 3b and 3c curve show high correlation with exponential and polynomial quadratic trend, respectively. Therefore, the viscosity shows an inverse correlation with T_2 (Fig. 3a), and all properties analyzed also exhibit the same relation. This is also due to the methyl ricinoleate: because it is unsaturated, an increase of its percentage in the blends favours an increase in the specific mass and the refractive index and should induce a viscosity reduction. However, the presence of the hydroxyl group increases the oil viscosity instead of reducing it.

The correlations shown in Figs. 2 and 3 also demonstrated that the NMR technique, based on the T_2 values of the samples, can be related to the physicochemical parameters of biodiesel. However, the correlations were constructed using a limited number of samples, more specifically of binary blends composed of the same biodiesel types (linseed/peanut and castor bean/soybean), where only the percentage of each one is changed. If the universe of the types of biodiesels and blends used in the correlations is expanded, the coefficients of determination (R^2) of the correlations decrease considerably. Thus, the PLS method was used to allow the expansion of biodiesel types in the same regression, generating smaller prediction errors of physicochemical properties than if simple correlations with T_2 were made.

3.3. PLS

The PLS method was used to calibrate of CPMG data (dependent variable) and the values of the quality parameters obtained by the experimental methods. The curves obtained by PLS, correlating the measured values by ASTM methods and predicted values of the PLS models, are shown in Fig. 4 and important information inherent to the models quality are given in Table 2. It is noteworthy that in the created models, the castor bean samples were eliminated by previous observations that show different tendencies from the others in such samples.

As can be seen from Table 2, four or five latent variables (LV) were used to perform the correlations. It is also verified that the cumulative variance was higher than 99.4% in all cases. In addition, the coefficients of determination (R^2) values of the calibration curves indicate the high linearity of the models and the low values of RMSEP are indicative of their accuracy. It is found that some samples deviated from the regression for the specific mass and for the refractive index (Fig. 4b and c), however, such deviations did not compromise the errors of prediction in a significant way. Together, such features demonstrate that the models created are very satisfactory and can predict the biodiesel properties from the CPMG data quite effectively.

In the prediction of viscosity, the RMSEP value was $0.1 \text{ mm}^2\text{s}^{-1}$. It is interesting to note that these RMSEP value is within reproducibility (R) of the ASTM D445 method, used to obtain the kinematic viscosity. R is equal to 2.24% of the measured values, ranging from $0.08 \text{ mm}^2\text{s}^{-1}$ for less viscous biodiesel (candlenut) to $0.12 \text{ mm}^2\text{s}^{-1}$ for the most viscous biodiesel (radish). The RMSEP value is also comparable to those found by Baptista et al. who developed a methodology for determining the specific mass and kinematic viscosity of biodiesel blends produced from soybean, palm, rapeseed and oil fry mixtures using near infrared (NIRS) spectroscopy in the range of $9000\text{--}4500 \text{ cm}^{-1}$. The authors constructed a PLS model that gave a RMSEP value for viscosity of $0.09 \text{ mm}^2\text{s}^{-1}$ [51].

For the specific mass determination, the model created resulted in RMSEP value of $3.7 \text{ kg}\cdot\text{m}^{-3}$. This result can also be compared to those obtained in other studies. Cunha et al. created a PLS method using medium infrared spectroscopy with Fourier transform and a horizontal attenuated total reflectance (HATR/m-FTIR) to predict the specific mass and refractive index of biodiesel and ternary and quaternary blends, from soybean, corn, sunflower and canola. The RMSEP value for the specific mass model was $0.2 \text{ kg}\cdot\text{m}^{-3}$ [13]. Ferrão et al., also using HATR/m-FTIR data, developed a PLS model with RMSEP value of

$0.73 \text{ kg}\cdot\text{m}^{-3}$ to determine the specific mass of blends of soybean biodiesel and diesel [52]. While in the previously mentioned article by Baptista et al. the RMSEP value for the specific mass was $0.9 \text{ kg}\cdot\text{m}^{-3}$ [51]. Although the RMSEP values of the models here generated are higher than those obtained in the cited works, they are still very satisfactory, since the range accepted by ANP for specific mass ($850\text{--}900 \text{ kg}\cdot\text{m}^{-3}$) has a variation of $50 \text{ kg}\cdot\text{m}^{-3}$.

For the refractive index prediction the RMSEP model value resulting was equal to 0.002. While Cunha et al. obtained the value of 0.0001 [13].

It is clear, then, based on the characteristics of the established models that from the generated data by CPMG, the capacities to predict the physicochemical properties of biodiesels by analyzing the biodiesel and blends samples. This verification, joined with the fact that the equipment of low-field NMR are bench-top, do not require any previous preparation of samples and the financial cost to maintain them is low, since they do not need cooling as the high field equipment, the technique stands out in the scope of use in quality laboratories in industries.

Models were also created only with pure biodiesel and blends of castor bean. Fig. 5 shows the curves correlating the measured values by ASTM methods and predicted values of the PLS models and important data related to the models quality are in Table 3. Three latent variables (LV) were used to perform the correlations and the cumulative variance was higher than 99.7% in all cases. The coefficients of determination (R^2) values indicate the high linearity of the models and the low values of RMSEP are an indication of their accuracy. Only a small deviation occurred in the refractive index regression (Fig. 5c), where the samples of pure castor bean biodiesel and the blends with high content of castor bean biodiesel (greater than 80%) move away of linearity, but this not interfered significantly with the model prediction errors. The RMSEP values for viscosity, specific mass and refractive index were, respectively, $0.6 \text{ mm}^2\text{s}^{-1}$, $2.0 \text{ kg}\cdot\text{m}^{-3}$ and 0.0005.

The high viscosity of castor bean biodiesel is an obstacle to its use as a fuel, not only in pure samples (B100), but also in blends with diesel. However, the blends formation with other biodiesels may be a solution to make them feasible. In this sense, the models obtained by PLS, created with the data generated by CPMG, proved to be highly significant to evaluate the parameters of blends containing castor bean biodiesel as one of its constituents.

4. Conclusions

The CPMG pulse sequence was associated with PLS regression and used to predict the physicochemical properties of biodiesel and blends. The kinematic viscosity, the specific mass and the refractive index could be determined with acceptable accuracy.

It was necessary to separate the set of samples into two distinct groups to create the PLS models. One group contained biodiesel and blends without castor bean and the other with castor bean, since the castor bean blends exhibited different correlations between their T_2 values and physicochemical properties.

RMSEP values for the viscosity, specific mass and refractive index were equal to $0.1 \text{ mm}^2\text{s}^{-1}$, $3.7 \text{ kg}\cdot\text{m}^{-3}$ and 0.002, respectively, for samples of biodiesel and blends without castor bean and $0.6 \text{ mm}^2\text{s}^{-1}$,

Table 2

Summary of the statistical parameters that describe the PLS models (Fig. 4) of each physicochemical property for pure biodiesel and blends without castor bean.

Curve	Property	Number of LV	Captured Variance (%)	R^2	RMSEP
a	Viscosity	4	99.45	0.9432	$0.1 \text{ mm}^2\text{s}^{-1}$
b	Specific Mass	4	99.45	0.9422	$3.7 \text{ kg}\cdot\text{m}^{-3}$
c	Refractive Index	5	99.47	0.9914	0.002

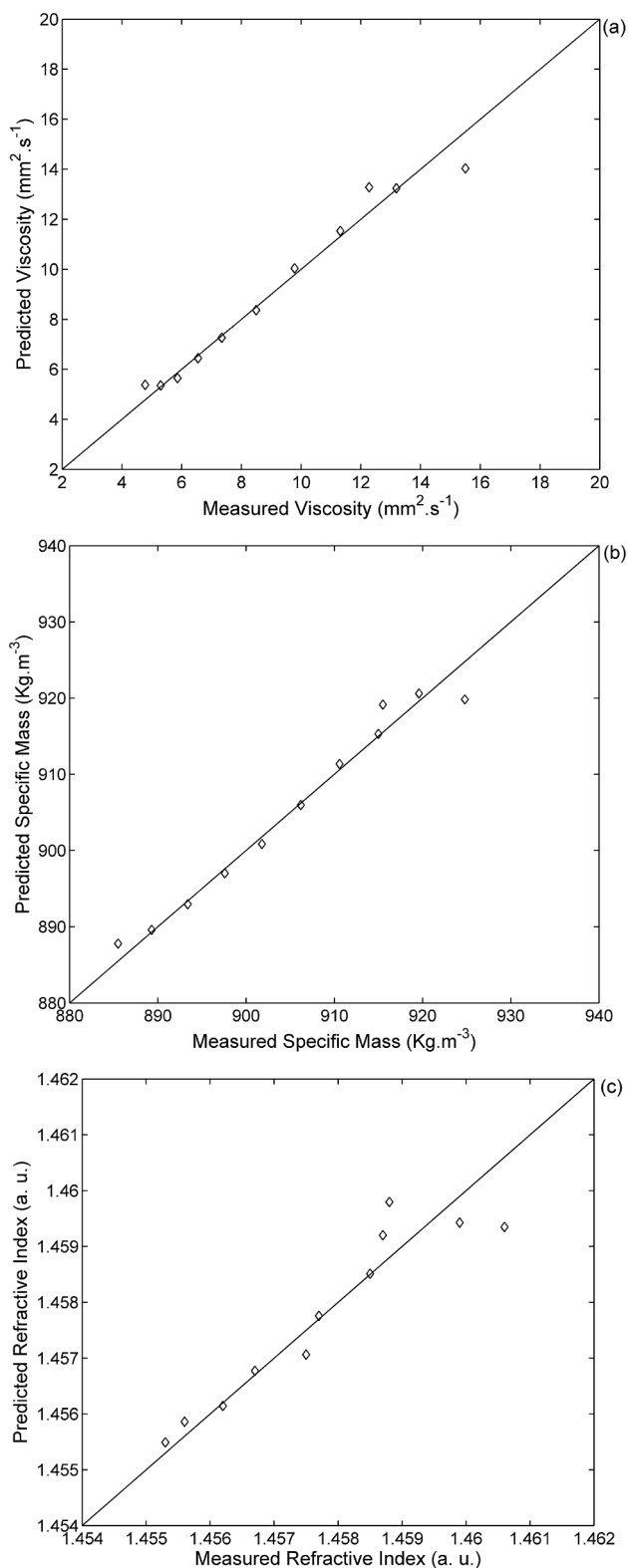


Fig. 5. Measured physicochemical properties by ASTM methods and its predicted values from the constructed PLS models: (a) viscosity; (b) specific mass; and (c) refractive index. The CPMG data used to build the models were generated from analyses of pure biodiesel and blends with castor bean.

Table 3

Summary of the statistical parameters that describe the PLS models (Fig. 5) of each physicochemical property for pure biodiesel and blends with castor bean.

Curve	Property	Number of LV	Captured Variance (%)	R ²	RMSEP
a	Viscosity	3	99.75	0.9715	0.6 mm ² .s ⁻¹
b	Specific Mass	3	99.75	0.9727	2.0 kg.m ⁻³
c	Refractive Index	3	99.76	0.8874	0.0005

2.0 kg.m⁻³ and 0.0005 for samples of biodiesel and blends with castor bean.

Acknowledgements

The authors would like to acknowledge CAPES (Coordenação de Aperfeiçoamento Pessoal de Nível Superior), CNPq (Conselho Nacional de Pesquisa), FAPES (Fundação de Amparo à Pesquisa e Inovação do Espírito Santo) and NCQP (Núcleo de Competências em Química do Petróleo) for their financial and technical support.

Appendix A. Supplementary data

Supplementary data to this article can be found online at <https://doi.org/10.1016/j.fuel.2018.10.045>.

References

- [1] Meher LC, Sagar DV, Naik SN. Technical aspects of biodiesel production by esterification – a review. *Renewable Sustainable Energy Rev* 2006;10:248–68.
- [2] Atadashi IM, Aroua MK, Aziz AA. High quality biodiesel and its diesel engine application: a review. *Renewable Sustainable Energy Rev* 2010;14:1999–2008.
- [3] Mahmudul HM, Hagos FY, Mamat R, Adam AA, Ishak WFW, Alenezi R. Production, characterization and performance of biodiesel as an alternative fuel in diesel engines – a review. *Renewable Sustainable Energy Rev* 2017;72:497–509.
- [4] Altin R, Çetinkaya S, Yücesu HS. The potential of using vegetable oil fuels as fuel for diesel engines. *Energy Convers Manage* 2001;42:529–38.
- [5] Rakoupolos CD, Antonopoulos KA, Rakoupolos DC, Hountalas DT, Giakoumis EG. Comparative performance and emissions study of a direct injection diesel engine using blends of diesel fuel with vegetable oils or bio-diesels of various origins. *Energy Convers Manage* 2006;47:3272–87.
- [6] Deepanraj B, Dhanesh C, Senthil R, Kannan M, Santhoshkumar A, Lawrence P. Use of palm oil biodiesel blends as a fuel for compression ignition engine. *Am J Appl Sci* 2011;8(11):1154–8.
- [7] Sharma S, Singh R, Mishra M, Mitra GK, Gangwar RK. Performance and emission analysis of diesel engine using biodiesel and preheated jatropha oil. *Int J Curr Res Acad Rev* 2014;2(6):229–39.
- [8] Shirmeshan A, Samani BH, Ghobadian B. Optimization of biodiesel percentage in fuel mixture and engine operating conditions for diesel engine performance and emission characteristics by Artificial Bees Colony Algorithm. *Fuel* 2016;184:518–26.
- [9] Prestes RA, Colnago LA, Forato LA, Vizzotto L, Novotny EH, Carrilho E. A rapid and automated low resolution NMR method to analyze oil quality in intact oilseeds. *Anal Chim Acta* 2007;596:325–9.
- [10] Knothe G. Dependence of biodiesel fuel properties on the structure of fatty acid alkyl esters. *Fuel Process Technol* 2005;86:1059–70.
- [11] Knothe G, Steidley KR. Kinematic viscosity of biodiesel fuel components and related compounds. Influence of compound structure and comparison to petrodiesel fuel components. *Fuel* 2005;84:1059–65.
- [12] Alptekin E, Canakci M. Determination of the density and the viscosities of biodiesel–diesel fuel blends. *Renewable Energy* 2008;33:2623–30.
- [13] Cunha CL, Luna AS, Oliveira RCG, Xavier GM, Paredes MLL, Torres AR. Predicting the properties of biodiesel and its blends using mid-FT-IR spectroscopy and first-order multivariate calibration. *Fuel* 2017;204:185–94.
- [14] Agência Nacional do Petróleo Gás Natural e Biocombustíveis (ANP). ANP Resolution No. 45 of August 2014. www.anp.gov.br [accessed on August 3rd, 2017].
- [15] Constantino AF, Lacerda Júnior V, Santos RB, Greco SJ, Silva RC, Neto AC, et al. Análise do teor e da qualidade dos lipídeos presentes em sementes de oleaginosas por RMN de baixo campo. *Quim Nova* 2014;37(1):10–7.
- [16] Rocha G, Colnago LA, Moraes TB, Zagonel GF, Muniz GIB, Peralta-Zamora PG, et al. Determination of biodiesel content in diesel fuel by time-domain nuclear Magnetic resonance (TD-NMR) spectroscopy. *Energy Fuels* 2017;31:5120–5.
- [17] Conway TF, Moffett GM, Earle FR. Nuclear magnetic resonance for oil content of seeds determining. *J Am Oil Chem Soc* 1963;40:265–8.
- [18] Colnago LA, Engelsberg M, Souza AA, Barbosa LL. High-throughput, non-

- destructive determination of oil content in intact seeds by continuous wave-free precession NMR. *Anal Chem* 2007;79:1271–4.
- [19] Van Duynhoven J, Voda A, Witek M, Van As H. Time-domain NMR applied to food products. *Annu Rep NMR Spectrosc* 2010;69:145–97.
- [20] Bertram HC, Andersen HJ, Karlsson AH. Comparative study of low-field NMR relaxation measurements and two traditional methods in the determination of water holding capacity of pork. *Meat Sci* 2001;57:125–32.
- [21] Engelsen SB, Jensen MK, Pedersen HT, Nørgaard L, Munck L. NMR-baking and multivariate prediction of instrumental texture parameters in bread. *J Cereal Sci* 2001;33:59–69.
- [22] Pedersen HT, Ablett S, Martin DR, Mallett MJD, Engelsen SB. Application of the NMR-MOUSE to food emulsions. *J Magn Reson* 2003;165:49–58.
- [23] Bertram HC, Whittaker AK, Andersen HJ, Karlsson AH. pH dependence of the progression in NMR T2 relaxation times in post-mortem muscle. *J Agric Food Chem* 2003;51:4072–8.
- [24] Hernández-Sánchez N, Hills BP, Barreiro P, Marigheto N. An NMR study on internal browning in pears. *Postharvest Biol Technol* 2007;44:260–70.
- [25] Maria RM, Colnago LA, Forato LA, Bouchard D. Fast and simple nuclear magnetic resonance method to measure conjugated linoleic acid in beef. *J Agric Food Chem* 2010;58:6562–4.
- [26] Ribeiro FZ, Marconcini LV, Toledo IB, Azeredo RBV, Barbosa LL, Colnago LA. Nuclear magnetic resonance water relaxation time changes in bananas during ripening: a new mechanism. *J Sci Food Agric* 2010;90:2052–7.
- [27] Pereira FMV, Carvalho AS, Cabeça LF, Colnago LA. Classification of intact fresh plums according to sweetness using time-domain nuclear magnetic resonance and chemometrics. *Microchem J* 2013;108:14–7.
- [28] Flores DWM, Colnago LA, Ferreira MD, Spoto MHF. Prediction of Orange juice sensorial attributes from intact fruits by TD-NMR. *Microchem J* 2016;128:113–7.
- [29] Santos PM, Kock FVC, Santos MS, Lobo CMS, Carvalho AS, Colnago LA. Non-invasive detection of adulterated olive oil in full bottles using time-domain NMR relaxometry. *J Braz Chem Soc* 2017;28(2):385–90.
- [30] Andrade FD, Colnago LA. Uso da RMN como um sensor *online* em processos industriais. *Quim Nova* 2012;35:2019–24.
- [31] Andrade FD, Netto AM, Colnago LA. Qualitative analysis by online nuclear magnetic resonance using Carr–Purcell–Meiboom–Gill sequence with low refocusing flip angles. *Talanta* 2011;84:84–8.
- [32] Morgan VG, Barbosa LL, Lacerda Júnior V, Castro EVR. Evaluation of the physicochemical properties of the postsalt crude oil for low-field NMR. *Ind Eng Chem Res* 2014;53:8881–9.
- [33] Goelman G, Prammer MG. The CPMG pulse sequence in strong magnetic field gradients with applications to oil-well logging. *J Magn Reson* 1995;113:11–8.
- [34] Fleury M, Deflandre F, Godefroy S. Validity of permeability prediction from NMR measurements. *C R Acad Sci Paris* 2001;4:869–72.
- [35] Hürlimann MD, Venkataramanan L. Quantitative measurement of two-dimensional distribution functions of diffusion and relaxation in grossly inhomogeneous fields. *J Magn Reson* 2002;157:31–42.
- [36] Guan H, Brougham D, Sorbie KS, Packer KJ. Wettability effects in a sandstone reservoir and outcrop cores from NMR relaxation time distributions. *J Pet Sci Eng* 2002;34:35–54.
- [37] Barbosa LL, Sad CMS, Morgan VG, Figueiras PR, Castro ERV. Application of low field NMR as an alternative technique to quantification of total acid number and sulphur content in petroleum from Brazilian reservoirs. *Fuel* 2016;176:146–52.
- [38] Barbosa LL, Kock FVC, Silva RC, Freitas JCC, Lacerda Júnior V, Castro EVR. Application of low-field NMR for the determination of physical properties of petroleum fractions. *Energy Fuels* 2013;27:673–9.
- [39] Meiboom S, Gill D. Modified spin-echo method for measuring nuclear relaxation times. *Rev Sci Instrum* 1958;29(8):688–91.
- [40] Flores IS, Godinho MS, Oliveira AE, Alcantara GB, Monteiro MR, Menezes SMC, Lião LM. Discrimination of biodiesel blends with ¹H NMR spectroscopy and principal component analyses. *Fuel* 2012;99:40–4.
- [41] Andersson M. A comparison of nine PLS1 algorithms. *J Chemom* 2009;23:518–29.
- [42] Kumar K, Mishra AK. Quantification of ethanol in ethanol-petrol and biodiesel in biodiesel-diesel blends using fluorescence spectroscopy and multivariate methods. *J Fluoresc* 2012;22:339–47.
- [43] Rodrigues EVA, Silva SRC, Romão W, Castro EVR, Figueiras PR. Determination of crude oil physicochemical properties by high-temperature gas chromatography associated with multivariate calibration. *Fuel* 2018;220:389–95.
- [44] Rocha WFC, Vaz BG, Sarmanho GF, Leal LHC, Nogueira R, Silva VF, et al. Chemometric techniques applied for classification and quantification of binary biodiesel/diesel Blends. *Anal Lett* 2012;45:2398–411.
- [45] Filzmoser P, Liebmann B, Varmuza K. Repeated double cross validation. *J Chemom* 2009;23:160–71.
- [46] Correia RM, Domingos E, Cáo VM, Araujo BRF, Sena S, Pinheiro LU, et al. Portable near infrared spectroscopy applied to fuel quality control. *Talanta* 2018;176:26–33.
- [47] Claridge TDW. *High-Resolution NMR. Techniques in Organic Chemistry*. second ed. Amsterdam: Elsevier; 2009.
- [48] Ba S, Zhang H, Lee YJ, Ng CW, Li T. Chemical modifications of ricinolein in castor oil and methyl ricinoleate for viscosity reduction to facilitate their use as biodiesels. *Eur J Lipid Sci Technol* 2016;118:651–7.
- [49] Knothe G. “Designer” biodiesel: optimizing fatty ester composition to improve fuel properties. *Energy Fuels* 2008;22:1358–64.
- [50] Chuck CJ, Bannister CD, Hawley JG, Davidson MG, Bruna IL, Paine A. Predictive model to assess the molecular structure of biodiesel fuel. *Energy Fuels* 2009;23:2290–4.
- [51] Baptista P, Felizardo P, Menezes JC, Correia MJN. Multivariate near infrared spectroscopy models for predicting the iodine value, CFPP, kinematic viscosity at 40 °C and density at 15 °C of biodiesel. *Talanta* 2008;77:144–51.
- [52] Ferrão MF, Viera MS, Pazos REP, Fachini D, Gerbase AE, Marder L. Simultaneous determination of quality parameters of biodiesel/diesel blends using HATR-FTIR spectra and PLS, iPLS or siPLS regressions. *Fuel* 2011;90:701–6.